Online Capacity Estimation of Lithium-ion Batteries by Partial Incremental Capacity Curve

Yixiu Wang
Department of Chemical and Biological Engineering
The University of British Columbia
Vancouver, Canada

Jiangong Zhu
Clean Energy Automotive Engineering Center
Tongji University
Shanghai, China

Liang Cao
Department of Chemical and Biological Engineering
The University of British Columbia
Vancouver, Canada

Bhushan Gopaluni
Department of Chemical and Biological Engineering
The University of British Columbia
Vancouver, Canada
Email: bhushan.gopaluni@ubc.ca

Yankai Cao
Department of Chemical and Biological Engineering
The University of British Columbia
Vancouver, Canada
Email: yankai.cao@ubc.ca

***Abstract*—Accurate capacity estimation is critical to ensure the safe and reliable usage of lithium-ion batteries, and data-driven methods are a promising technique for this task. However, the existing studies require the whole charging curve for feature extraction and usage of sophisticated machine learning methods, which are not suitable for online applications. This paper proposes a simple machine learning technique, partial least squares regression, for online battery capacity estimation based on the partial incremental capacity curve. The features can be easily obtained by interpolation of the measured charging profile without data smoothing, leading to a low computational cost. The proposed method is realized and tested on three battery datasets (#5, #7, #18) provided by NASA. Experimental results show that the model trained on 80% of the data samples of cell #5 can achieve a 0.01053Ah root mean squared error for the remaining 20% data of cell #5. The model is further verified on the other two battery datasets without changing model weights, and the test root mean squared error is 0.02046Ah for cell #7 and 0.02700Ah for cell #18, indicating the generality of the proposed capacity estimation method.**

***Index Terms*—lithium-ion batteries, capacity estimation, partial least squares regression, incremental capacity curve**

I. INTRODUCTION

Nowadays, lithium-ion batteries have been the dominant power sources for electric vehicles, portable electronic devices and other applications because of their high energy and power density [1]. However, battery degradation over time poses a significant challenge in the use of lithium-ion batteries, which leads to degraded performance and potentially higher operating costs [2]. State of Health (SOH) is an indicator of the internal performance of the battery, and it is usually expressed by capacity. Typically, the battery capacity is calculated by integrating the discharging current from a complete discharging process of a fully charged battery, but the complete discharging process is usually unavailable due to the uncertainties in environmental and operational conditions [3]. For the safe and reliable usage of lithium-ion batteries, it is critical to accurately estimate the capacity through the partial charging curve in real-time.

Many research efforts have been conducted to do capacity estimation from the voltage and current measurements in the last decades. These capacity estimation methods are based on the relationship between the electricity charged or discharged from the battery and the voltage difference before and after the corresponding process [4], and they can be divided into two main categories, namely model-based methods and data-driven methods. The equivalent circuit model (ECM) [5] is a common model used in the model-based capacity estimation methods, which simulates the behaviour of a battery with a combination of simple electronic components such as resistors and capacitors. After establishing the battery state-space equations by utilizing ECM, some recursive adaptive filters such as the extended Kalman filter (EKF) [6] [7] and particle filter (PF) [8] have been adopted to identify model parameters and update battery capacity. For example, Plett et al. [6] proposed a dual EKF method to simultaneously estimate the State of Charge (SOC) and capacity of the battery. The experimental results show that capacity estimation has converged to the correct value and exhibits little variation over time. Although the model-based capacity estimation methods can achieve high accuracy, but they are computationally intensive and are not suitable for online applications.

In recent years, data-driven methods have become popular in the research field of batteries and they can reflect the intrinsic correlation between the measurements and the battery SOH without expert knowledge on aging mechanisms. A wealth of machine learning approaches have been used for capacity estimation including Gaussian process regression (GPR) [9] [10], relevance vector machine (RVM) [11], deep neural networks (DNNs) [12], random forest regression (RFR) [13], etc. To estimate battery capacity accurately, it is critical to extract representative features as input for the data-driven methods.

Zhang et al. [9] introduced a capacity estimation method by combining the electrochemical impedance spectroscopy (EIS) spectrum with GPR. However, the real-time acquisition of the EIS spectrum is still a challenge in a real-life usage scenario of EVs. Ref. [10]–[12] use the features extracted from the charging process to estimate the capacity and achieve high accuracy. One limitation of these methods is that they require the use of a whole charging curve to obtain health features, which is not guaranteed during the vehicle operation. Yi et al. [13] proposed an RFR with 500 regression trees for battery capacity estimation based on the features extracted from the partial constant current (CC) charging curve. However, the proposed RFR itself is a complex algorithm and suffers from intensive computation, which is not suitable for online use. Moreover, the complex structure of RFR makes the need for more data to train the model to reduce overfitting and collecting a large amount of data is time-consuming in practice. Therefore, it is necessary to develop a simple regression model for online capacity estimation.

This paper proposes a simple machine learning technique, partial least squares regression (PLSR), for online capacity estimation based on the partial incremental capacity (IC) curve. The remainder of the paper is organized as follows. Section II gives out the cycling dataset of the study, and Section III introduces the proposed methodology. The estimation results and discussion are reported in Section IV and finally, some conclusions are drawn in Section V.

II. Cycling Dataset

To evaluate the performance of the proposed battery capacity estimation method, a cycling dataset of three commercial 18650-size lithium-ion battery cells with the same type (#5, #7, #18) from the Prognostics Center of Excellence(PCoE) at Ames Research Center, NASA [14] is used in this work. These batteries were run through 3 different operational profiles (charging, discharging and impedance) at room temperature of 24 °C. The charging process was performed in a CC mode at 1.5A until the battery voltage reached 4.2V, followed by a constant voltage (CV) charging step at 4.2V until the current dropped to 20mA. The discharging process was carried out in a CC mode at 2A until the battery voltage fell to 2.7V, 2.2V and 2.5V for cells #5, #7 and #18, respectively, and battery capacity was obtained by integration of the discharge current starting from a completely charged battery to the battery voltage dropped to 2.7V. Impedance measurement was conducted through an EIS frequency sweep from 0.1Hz to 5kHz, which can provide insight into the battery's internal parameters. The repetitive cycles of the charging and discharging process resulted in accelerated degradation of the batteries, and the experiment was stopped when the battery capacity reached end-of-life (EOL) criteria, which was a 30% fade in nominal capacity (from 2Ah to 1.4Ah).

Fig. 1 shows the change of battery capacity with cycle number for experimental cells. It is clear that as the number of cycles increases, the battery capacity shows an overall decreasing trend, suggesting that the repeated charging and discharging process leads to irreversible physical and chemical changes within the battery. It can also be noticed that the three batteries exhibit different degradation characteristics, with cell #18 showing the fastest capacity fade rate and cell #7 showing the slowest capacity fade rate, indicating that different cut-off voltages have a significant effect on battery degradation. Moreover, the curves in the figure also demonstrate that different cells have different values of capacity for the same number of cycles, which means that it is not practical to estimate capacity directly using the cycle number. Thus, it is necessary to use other cycling information, such as measurements from the charging process, for battery capacity estimation.

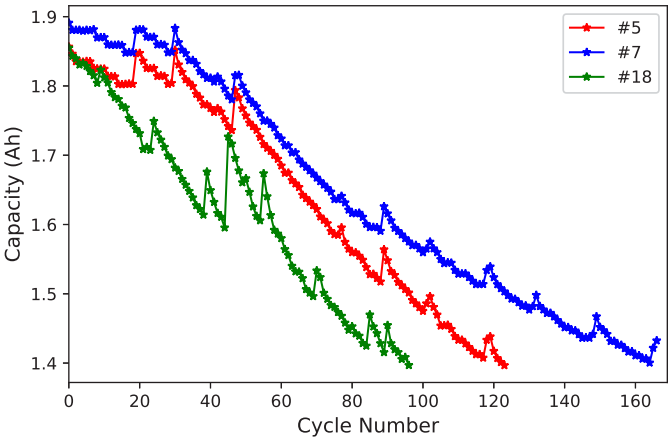

Fig. 1. Capacity change of three experimental batteries.

III. Methodology

A. Partial incremental capacity curve

Incremental capacity (IC) is the differentiation of the change in battery capacity over the change in terminal voltage, and IC analysis is a powerful tool to study the degradation mechanism of lithium-ion batteries. Each peak of the IC curves indicates a specific electrochemical process within the cell, thus many previous studies have used the peak position [15] and peak intensity [16] of IC curves as features to estimate battery capacity and achieved high accuracy. However, one drawback of IC analysis is that it is very sensitive to data noise, and the measurement noise of the battery system often makes the peaks of the IC curve not easily identified. Typically, proper data smoothing methods, such as the Gaussian filter, have to be employed to obtain a smooth IC curve, but it is hard to implement for online applications due to the limited computational capability of the present battery management system (BMS). In this paper, we propose to estimate the battery capacity directly using the IC values for a specific voltage region, with no need for data smoothing.

In reality, BMS samples current and voltage at equal time intervals, which does not guarantee the same sampling points for a specific voltage region over all cycles. In order to have fixed length input features for the model, an interpolation-based IC curve acquisition algorithm is proposed in this paper.

More specifically, considering the CC charging profile shown in Fig. 2, it can be expressed as $\mathcal{D}^m = \{(t_i^m, I_i^m, V_i^m), i = 1, 2, \cdots, n^m\}$, where I_i^m and V_i^m are the measured current and voltage at the sampling time point t_i^m, and n^m is the total number of sampling points. For a specific voltage region from V_l to V_h, it can be discretized with ΔV interval to get the desired $\mathcal{V} = \{V_l, V_l + \Delta V, \cdots, V_h\} = \{V_i, i = 1, 2, \cdots, k\}$, where the number of discrete points k can be calculated by $k = (V_h - V_l)/\Delta V + 1$. Then the time t_i to have the desired V_i in V can be obtained by interpolating the two nearest voltage measurements V_i^m and V_{i+1}^m in $\mathcal{D}^m$, as shown in the following equation:

$$\frac{V_i - V_i^m}{V_{i+1}^m - V_i^m} = \frac{t_i - t_i^m}{t_{i+1}^m - t_i^m} \tag{1}$$

$$t_i = \frac{V_i - V_i^m}{V_{i+1}^m - V_i^m}(t_{i+1}^m - t_i^m) + t_i^m \tag{2}$$

Similarly, I_i can be calculated by the following equation:

$$I_i = \frac{V_i - V_i^m}{V_{i+1}^m - V_i^m}(I_{i+1}^m - I_i^m) + I_i^m \tag{3}$$

After we get the desired $\mathcal{I} = \{I_i, i = 1, 2, \cdots, k\}$ and $\mathcal{T} = \{t_i, i = 1, 2, \cdots, k\}$, IC at V_i can be approximated by

$$\left.\frac{dQ}{dV}\right|_{V_i} \approx \left.\frac{\Delta Q}{\Delta V}\right|_{V_i} = \frac{I_i(t_{i+1} - t_i)}{\Delta V} \tag{4}$$

Fig. 3 shows the IC curves for cycle 1 and cycle 100 of cell #5 when ΔV is 0.002V. As shown in the figure, we can notice that the IC values at cycle 1 are generally higher than those at cycle 100, the curves show a significant difference in the voltage range from 3.8V to 4.0V. Therefore, the specific voltage range selected in this work is 3.8V-4.0V.

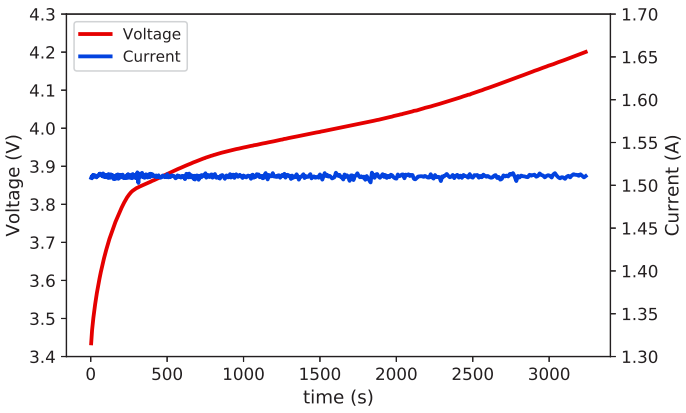

Fig. 2. Constant current charging profile for cycle 1 of cell #5.

B. Partial least squares regression

PLSR [17] is a generalization of the ordinary multiple linear regression (MLR), and it is very effective when the number of samples is smaller than the number of variables or when there is severe collinearity in the variables. In this section, I will give a brief introduction to PLSR.

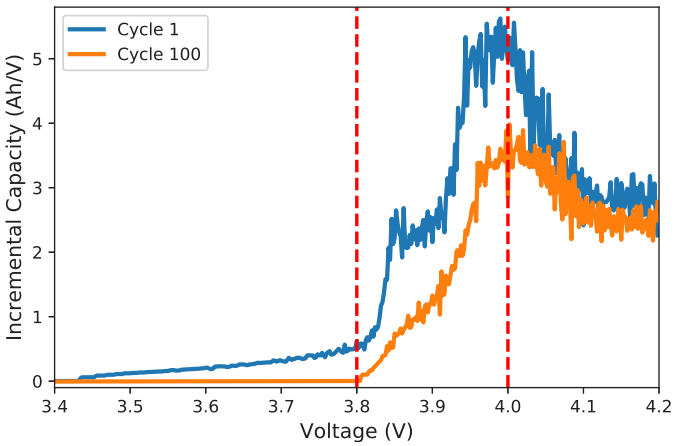

Fig. 3. Incremental capacity curves of cell #5.

To facilitate understanding of PLSR, let's start with MLR. Considering a regression problem with the features matrix $X = \{x_{ij}, i = 1, 2, \cdots, n, j = 1, 2, \cdots, p\}$ and the target $y = \{y_i, i = 1, 2, \cdots, n\}$, where n is the number of samples and p is the number of features, MLR establishes a linear relationship between them by

$$y = Xb + e \tag{5}$$

where b is the regression coefficient to be solved and e is the residual. We can solve b by least squares method and the solution is

$$b = (X'X)^{-1}X'y \tag{6}$$

When the data samples satisfy the Gauss–Markov theorem, (6) is effective to obtain an unbiased least squares estimation of b. However, small samples and colinearity often make it hard to obtain valid estimation of b. PLSR addresses this problem by projecting X and y into a low-dimensional space and then performing regression. The implementation details of PLSR are illustrated as follows.

PLSR starts with finding the first component c_1 of X with $c_1 = Xw_1$. By maximizing $Cov(c_1, y)$, we can solve the optimization problem to get

$$w_1 = \frac{X^T y}{||X^T y||}, c_1 = Xw_1 = \frac{XX^T y}{||X^T y||} \tag{7}$$

Then the regressions of X and y on c_1 are performed separately:

$$\begin{cases} X = c_1 p_1^T + X_1 \\ y = c_1 r_1 + y_1 \end{cases} \tag{8}$$

where the coefficients are

$$\begin{cases} p_1 = \dfrac{X^T t_1}{||t_1||^2} \\ r_1 = \dfrac{y^T t_1}{||t_1||^2} \end{cases} \tag{9}$$

In addition, X_1 and y are the residuals. By replacing X and y with X_1 and y_1 and repeating the above process, we can

obtain the other components c_i and the corresponding weights w_i, p_i and r_i, where $i = 2, \cdots, m$ and m is the number of components.

Considering that

$$\begin{aligned} c_i &= X_{i-1}w_i = X_{i-2}(E - w_{i-1}p_{i-1}^T)w_i \\ &= X\prod_{k=1}^{i-1}(E - w_k p_k^T)w_i \end{aligned} \tag{10}$$

we can let

$$w_i^* = \prod_{k=1}^{i-1}(E - w_k p_k^T)w_i \tag{11}$$

then we can have $c_i = Xw_i^*$ and

$$\begin{aligned} y &= c_1 r_1 + c_2 r_2 + \cdots + c_m r_m + y_m \\ &= Xw_1^* r_1 + Xw_2^* r_2 + \cdots + Xw_m^* r_m + y_m \\ &= X\left(\sum_{i=1}^{m} w_i^* r_i\right) + y_m = Xb + y_m \end{aligned} \tag{12}$$

where $b = \sum_{i=1}^{m} w_i^* r_i$ is the coefficient of PLSR.

IV. RESULTS AND DISCUSSIONS

A. Metrics

To evaluate the predictive performance of the proposed model, coefficient of determination (R^2) and root mean square error ($RMSE$) are used in this work, and they are given by

$$R^2 = 1 - \frac{\sum_{i=1}^{N}(Q_i - \hat{Q}_i)^2}{\sum_{i=1}^{N}(Q_i - \bar{Q})^2} \tag{13}$$

$$RMSE = \sqrt{\frac{1}{N}\sum_{i=1}^{N}(Q_i - \hat{Q}_i)^2} \tag{14}$$

where Q_i is the observed capacity, $\hat{Q}_i$ is the predicted capacity from the model, $\bar{Q}$ is the mean of the observed data and N is the total number of samples. For a model, R^2 close to 1 and $RMSE$ close to 0 indicate a good match between measured and predicted data.

B. Performance of the proposed model

In this work, the effectiveness of the proposed PLSR model is bench-marked with the other three commonly used machine learning models, including MLR, support vector regression (SVR) and random forest regression (RFR). MLR finds a linear relationship between the inputs and output. SVR is a special case of support vector machine in regression, which was designed to find the optimal decision boundary. RFR generates hundreds of independent decision trees and then averages the results of all decision trees to get the output. The input features of these models are the 100 IC values over a voltage range of 3.8V to 4.0V for any cycle, and the output is the corresponding capacity for that cycle. All models are trained on a randomly selected 80% of the cycling data of cell #5 and then are tested on the remaining 20% of the data. Moreover, to verify the generality of the proposed models, the models trained by data of cell #5 are also tested on data from cell #7 and cell #18 without changing model weights.

TABLE I compares the performance of different models. We can notice that MLR and SVR show poor prediction accuracy for all 3 test cases. One possible reason for the poor performance is that we have 100 features but only 98 training samples, and the number of features exceeds the number of samples making the model severely overfitted. For RFR, bootstrap aggregating and randomly selected features make it less prone to overfitting and thus it shows higher accuracy on the data samples from cell #5 and cell #7. In an attempt to deal with the overfitting problem caused by too many features for MLR and SVR, the correlation analysis is applied to do the feature selection. Fig. 4 demonstrates the Pearson correlation coefficient between capacity and features obtained by using the training data, where the variable 0 is the capacity. By selecting the 10 most relevant features to the capacity as new inputs, we can retrain MLR and SVR, and then evaluate their performance on the test dataset. We denote the new models MLR-FS and SVR-FS. From TABLE I, it is clear that the accuracy of MLR-FS is significantly improved compared to MLR for all 3 test cases, and SVR-FS also shows some improvement for the data samples of cell #5 and cell #7. However, we also notice that SVR-FS has a slight decrease in accuracy for the data samples of cell #18, because some information is lost in the simple feature selection.

TABLE I
PERFORMANCE COMPARISON OF DIFFERENT MODELS

Model	Cell #5		Cell #7		Cell #18	
	R^2	$RMSE$	R^2	$RMSE$	R^2	$RMSE$
MLR	0.7011	0.08336	0.6571	0.09384	0.1841	0.11893
MLR-FS	0.9878	0.01682	0.9268	0.04334	0.6093	0.08230
SVR	0.8080	0.06681	0.7518	0.07984	0.6898	0.07334
SVR-FS	0.8522	0.05861	0.7854	0.07423	0.4691	0.09594
RFR	0.9894	0.01572	0.9535	0.03456	0.4448	0.09811
PLSR	**0.9952**	**0.01053**	**0.9837**	**0.02046**	**0.9580**	**0.02700**

We also report the prediction performance of PLSR with 4 components. As shown in TABLE I, PLSR demonstrates the best accuracy in all 3 test cases. The test error for cell #5 achieves an $RMSE$ of 0.01053Ah, which reaches the accuracy of 0.010222Ah $RMSE$ obtained using the whole CC-CV charging curve in Ref. [11]. Ref. [11] also reports an estimated error of 0.041133Ah $RMSE$ for cell #18, which is worse than our performance, confirming the generality of our proposed model. The effectiveness of PLSR is expected, because Fig. 4 implies a severe colinearity between features, and PLSR is particularly suited for this case as it can project the original variables to latent structures. For the proposed PLSR, the predicted capacity versus observed capacity is illustrated in Fig. 5 for visualization purposes. Fig. 6 further demonstrates the distribution of prediction errors. As shown in

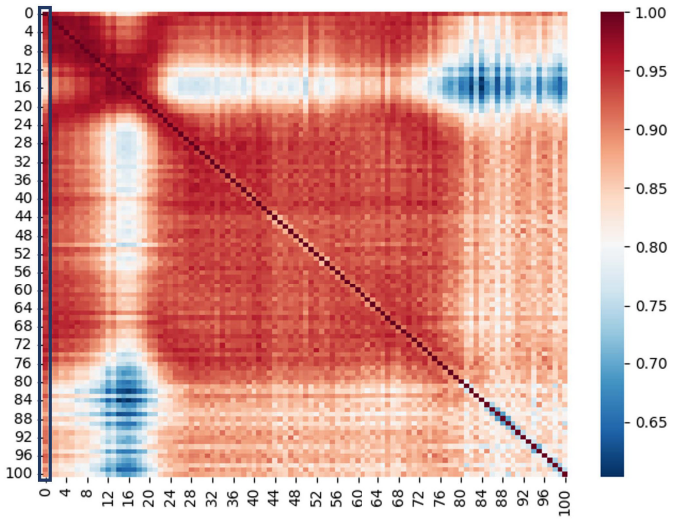

Fig. 4. The result of correlation analysis between capacity and IC values.

Fig. 6(a), the prediction errors for data samples of cell #5 are all within 0.02Ah, which corresponds to 1% of the relative error to the nominal capacity. For data samples of cell #7, Fig. 6(b) shows that the errors are mostly concentrated within 0.03Ah (1.5%), with only a few samples reaching 0.06Ah (3%). From Fig. 6(c), it is clear that the prediction errors for data samples of cell #18 are significantly larger than the other two, with one sample reaching 0.15Ah (7.5%), but most of the samples are still in the range of 0.025Ah (1.25%).

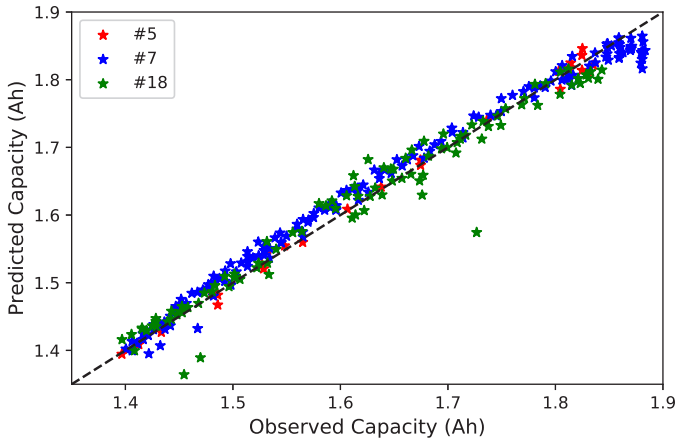

Fig. 5. Test results of predicted capacity versus observed capacity by PLSR.

C. Influence of the Number of Components of PLSR

To investigate the influence of the different number of components of PLSR on the prediction performance, TABLE II lists the accuracy of PLSR with the number of components from 1 to 10. It can be seen that as the number of components increases, the accuracy first demonstrates an upward trend, followed by a downward trend. It makes sense as too few components can cause a large amount of information to be

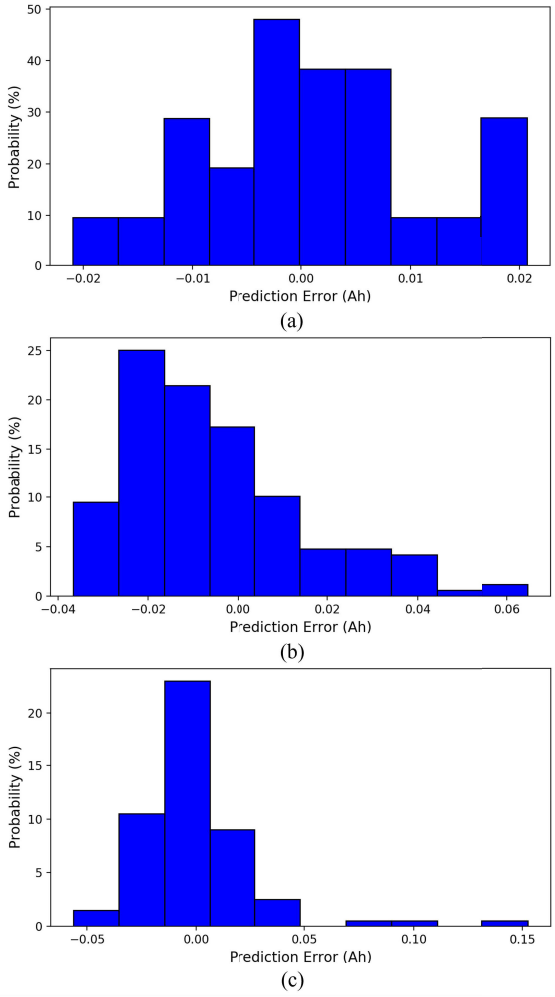

Fig. 6. Distribution of prediction errors. (a) For data samples of cell #5; (b) For data samples of cell #7; (c) For data samples of cell #18.

lost and thus reduce the model performance, while too many components can make the model more prone to overfitting. In our case, 4 components would result in the best prediction performance for data samples of cell #5 and cell #7, while 6 components would lead to the best prediction accuracy for data samples of cell #18.

TABLE II
PERFORMANCE COMPARISON WITH DIFFERENT NUMBER OF COMPONENTS

Number of components	Cell #5		Cell #7		Cell #18	
	R^2	$RMSE$	R^2	$RMSE$	R^2	$RMSE$
1	0.9932	0.01261	0.9677	0.02878	0.7262	0.06890
2	0.9935	0.01233	0.9655	0.02977	0.8565	0.04987
3	0.9944	0.01140	0.9792	0.02311	0.9488	0.02980
4	**0.9952**	**0.01053**	**0.9837**	**0.02046**	0.9580	0.02700
5	0.9941	0.01171	0.9835	0.02057	0.9576	0.02710
6	0.9924	0.01327	0.9827	0.02107	**0.9588**	**0.02672**
7	0.9907	0.01467	0.9820	0.02149	0.9580	0.02699
8	0.9898	0.01544	0.9815	0.02179	0.9545	0.02809
9	0.9886	0.01629	0.9805	0.02240	0.9514	0.02903
10	0.9878	0.01687	0.9794	0.02302	0.9487	0.02981

V. CONCLUSIONS

In this paper, a PLSR is proposed to estimate battery capacity based on the partial IC curve. Specifically, an interpolation-based IC curve acquisition algorithm is first proposed to approximate the IC value at desired voltage point from the measured charging profile in the voltage range from 3.8-4.0V, then a PLSR model is trained to learn the dependency of the battery capacity on the IC values. Three battery datasets (#5, #7, #18) from NASA are used to train and test the proposed model. Experimental results show that the PLSR model with 4 components trained on 80% data samples of cell #5 can achieve a 0.9952 R^2 and a 0.01053Ah $RMSE$ for the remaining 20% data samples. Moreover, the trained model obtains a 0.9837 R^2 and a 0.02046Ah $RMSE$ for data samples of cell #7 and a 0.9580 R^2 and a 0.02700Ah $RMSE$ for data samples of cell #18 without changing the model weights. The success of this work promotes the development of online battery estimation using data-driven methods.

ACKNOWLEDGMENT

Yankai Cao acknowledges funding from the discovery program of the Natural Science and Engineering Research Council of Canada under grant RGPIN-2019-05499. Bhushan Gopaluni would like to acknowledge the financial support from NSERC Discovery grant. We gratefully acknowledge the computing resources provided by SciNet (www.scinethpc.ca) and Compute Canada (www.computecanada.ca).

REFERENCES

[1] D. Bresser, K. Hosoi, D. Howell, et al. "Perspectives of automotive battery R&D in China, Germany, Japan, and the USA," J. Power Sources, vol. 382, pp. 176-178, 2018.

[2] X. Han, L. Lu, Y. Zheng, et al. "A review on the key issues of the lithium-ion battery degradation among the whole life cycle," transportation, vol. 1, pp. 100005, 2019.

[3] J. Zhu, Y. Wang, Y. Huang, et al. "Data-driven capacity estimation of commercial lithium-ion batteries from voltage relaxation," Nat. Commun., vol. 13, pp.1-10, 2022.

[4] W. Waag, C. Fleischer, D. U. Sauer, "Critical review of the methods for monitoring of lithium-ion batteries in electric and hybrid vehicles," J. Power Sources, vol. 258, pp.324-339, 2014.

[5] B. Y. Liaw, G. Nagasubramanian, R. G. Jungst, et al. "Modeling of lithium-ion cells—A simple equivalent-circuit model approach," Solid-state Ionics, vol. 175, no. 1-4, pp. 835-839, 2004.

[6] G. L. Plett, "Extended Kalman filtering for battery management systems of LiPB-based HEV battery packs: Part 3. State and parameter estimation," J. Power Sources, vol. 134, no. 2, pp. 277-292, 2004.

[7] C. Zou, C. Manzie, D. Nešić, et al. "Multi-time-scale observer design for state-of-charge and state-of-health of a lithium-ion battery," J. Power Sources, vol. 335, pp. 121-130, 2016.

[8] S. Schwunk, N. Armbruster, S. Straub, et al. "Particle filter for state of charge and state of health estimation for lithium–iron phosphate batteries," J. Power Sources, vol. 239, pp. 705-710, 2013.

[9] Y. Zhang, Q. Tang, Y. Zhang, et al. "Identifying degradation patterns of lithium-ion batteries from impedance spectroscopy using machine learning," Nat. Commun., vol. 11, pp. 1-6, 2020.

[10] D. Yang, X. Zhang, R. Pan, et al. "A novel Gaussian process regression model for state-of-health estimation of lithium-ion battery using charging curve," J. Power Sources, vol. 384, pp. 387-395, 2018.

[11] P. Guo, Z. Cheng, L. Yang, "A data-driven remaining capacity estimation approach for lithium-ion batteries based on charging health feature extraction." J. Power Sources, vol. 412, pp. 442-450, 2019.

[12] D. Roman, S. Saxena, V. Robu, et al. "Machine learning pipeline for battery state-of-health estimation," Nat. Mach. Intell., vol. 3, pp. 447-456, 2021.

[13] Y. Li, C. Zou, M. Berecibar, et al. "Random forest regression for online capacity estimation of lithium-ion batteries," Appl. Energy, vol. 232, pp. 197-210, 2018.

[14] B. Saha and K. Goebel. "Battery Data Set," NASA Ames Prognostics Data Repository, NASA Ames Research Center, Moffett Field, CA, 2007.

[15] Y. Li, M. Abdel-Monem, R. Gopalakrishnan, et al. "A quick on-line state of health estimation method for Li-ion battery with incremental capacity curves processed by Gaussian filter," J. Power Sources, vol. 373, pp. 40-53, 2018.

[16] C. Weng C, Y. Cui, J. Sun, et al. "On-board state of health monitoring of lithium-ion batteries using incremental capacity analysis with support vector regression," J. Power Sources, vol. 235, pp. 36-44, 2013.

[17] S. Wold, M. Sjöström, L. Eriksson, "PLS-regression: a basic tool of chemometrics," Chemometrics and intelligent laboratory systems, vol. 58, no.2, pp.109-130, 2001.